Journal of Anatomy

J. Anat. (2013) **222**, pp437–450 doi: 10.1111/joa.12032

Isolation, characterization and the multi-lineage differentiation potential of rabbit bone marrow-derived mesenchymal stem cells

Sik-Loo Tan,[1] Tunku Sara Ahmad,[1] Lakshmi Selvaratnam[2] and Tunku Kamarul[1]

[1]*Tissue Engineering Group, National Orthopaedics Centre of Excellence in Research & Learning, Department of Orthopaedic Surgery, Faculty of Medicine, University of Malaya, Kuala Lumpur, Malaysia*
[2]*School of Medicine & Health Sciences, Monash University, Sunway Campus, Subang Jaya, Selangor, Malaysia*

Abstract

Mesenchymal stem cells (MSCs) are recognized by their plastic adherent ability, fibroblastic-like appearance, expression of specific surface protein markers, and are defined by their ability to undergo multi-lineage differentiation. Although rabbit bone marrow-derived MSCs (rbMSCs) have been used extensively in previous studies especially in translational research, these cells have neither been defined morphologically and ultrastructurally, nor been compared with their counterparts in humans in their multi-lineage differentiation ability. A study was therefore conducted to define the morphology, surface marker proteins, ultrastructure and multi-lineage differentiation ability of rbMSCs. Herein, the primary rbMSC cultures of three adult New Zealand white rabbits (at least 4 months old) were used for three independent experiments. rbMSCs were isolated using the gradient-centrifugation method, an established technique for human MSCs (hMSCs) isolation. Cells were characterized by phase contrast microscopy observation, transmission electron microscopy analysis, reverse transcriptase-polymerase chain reaction (PCR) analysis, immunocytochemistry staining, flow cytometry, alamarBlue® assay, histological staining and quantitative (q)PCR analysis. The isolated plastic adherent cells were in fibroblastic spindle-shape and possessed eccentric, irregular-shaped nuclei as well as rich inner cytoplasmic zones similar to that of hMSCs. The rbMSCs expressed CD29, CD44, CD73, CD81, CD90 and CD166, but were negative (or dim positive) for CD34, CD45, CD117 and HLD-DR. Despite having similar morphology and phenotypic expression, rbMSCs possessed significantly larger cell size but had a lower proliferation rate as compared with hMSCs. Using established protocols to differentiate hMSCs, rbMSCs underwent osteogenic, adipogenic and chondrogenic differentiation. Interestingly, differentiated rbMSCs demonstrated higher levels of osteogenic (*Runx2*) and chondrogenic (*Sox9*) gene expressions than that of hMSCs ($P < 0.05$). There was, however, no difference in the adipogenic (*Ppar*γ) expressions between these cell types ($P > 0.05$). rbMSCs possess similar morphological characteristics to hMSCs, but have a higher potential for osteogenic and chondrogenic differentiation, despite having a lower cell proliferation rate than hMSCs. The characteristics reported here may be used as a comprehensive set of criteria to define or characterize rbMSCs.

Key words: cell differentiation; cell therapy; mesenchymal stem cells; orthopaedics; tendon; tissue engineering.

Introduction

Mesenchymal stem cells (MSCs) are multipotent cells that can undergo multi-lineage differentiation. Due to this, many studies have been conducted with the ultimate aim to harness the potential of these cells for many possible applications, especially for translational research (Dashtdar et al. 2011; Tay et al. 2011). The use of rabbit MSCs (rbMSCs) has been described in many previous studies, and has recently been very popular with many scientists, due to a readily available supply of this animal. Furthermore, it has been described that these cells possess cellular and tissue physiology that closely resemble human

Correspondence
Sik-Loo Tan, Tissue Engineering Group, National Orthopaedics Centre of Excellence in Research & Learning, Department of Orthopaedic Surgery, Faculty of Medicine, University of Malaya, Kuala Lumpur, Malaysia. E: tansikloo@yahoo.com

Presented in abstract form at the 2009 International Society for Stem Cell Research (ISSCR) 7th Annual Meeting, Barcelona, Spain, July 2009. This manuscript also represents a portion of a thesis to be submitted by S.-L. Tan to the Department of Orthopaedic Surgery, University of Malaya as partial fulfillment of the requirements for a PhD degree
Accepted for publication *28 January 2013*

MSCs (hMSCs; Fox, 1984; Warden, 2007). In *in vivo* models, the rabbit has the advantage over other animals due to its relatively larger size compared with the rat or mouse. It is inexpensive and is relatively easy to handle compared with other larger animal models, such as dogs, goats or sheep. However, unlike hMSCs, there is not much in the literature about the basic characteristics that define rbMSCs (Gupta & Lee, 2007; Warden, 2007; Amini et al. 2012). Despite being readily available, many researchers are in a dilemma when it comes to using rbMSCs as the validity of studies conducted using these cells may be questioned. This is especially true because rbMSCs, until today, remain largely undefined. Furthermore, whilst these cells may have certain potentials that mimic MSCs, they may in fact be merely progenitor cells that may have been isolated during the harvesting process (Chong et al. 2011). This further creates other issues as the outcome of many experiments may turn out to be unreliable because the cell population used would then be of a mixed type. It is therefore imperative that the identification and characterization of MSCs from different tissue origins (Koerner et al. 2006; Laitinen & Laine, 2007; Bunnell et al. 2008) or different species (Zeng et al. 2006; Nadri et al. 2007; Neupane et al. 2008) must be clearly defined in order to validate any studies in which they are used.

According to the International Society for Cellular Therapy (ISCT), MSCs are defined as cells that are: (i) plastic adherent; (ii) express CD105, CD73 and CD90, whilst lacking in the expression of CD45, CD34, CD14 or CD11b, CD79α or CD19 and HLA-DR surface molecules; and (iii) can differentiate into osteogenic, chondrogenic and adipogenic lineages (Dominici et al. 2006). In previous literature, MSCs obtained from rabbits have been shown to be able to adhere to plastic surfaces and undergo tri-lineage differentiation (Owen et al. 1987; Sahoo et al. 2010). Although MSC surface protein markers have been reported extensively in human (Chamberlain et al. 2007; Haasters et al. 2009), murine (Tropel et al. 2004; Nadri et al. 2007) and rodent (Marcus et al. 2008; Karaoz et al. 2009) cells, identification of these cells in other animal models such as rabbit (Amini et al. 2012) has not been widely published. This is mainly due to the lack of molecular biology information and the limited availability of the monoclonal antibodies (mAbs) necessary for the characterization of these cells. Furthermore, there have not been any studies that have made a comparison between the ability of rbMSCs to express various differentiation genes, for example osteogenic or chondrogenic, as compared with hMSCs. This information is important because many studies, such as those of translational models, would require the fundamental understanding of the differences between these two sources to ensure accurate interpretation of the data obtained.

This study was therefore conducted to isolate and characterize rbMSCs isolated using a commonly practiced method described by the majority of studies, i.e. gradient centrifugation technique. These cells are then identified and recognized through: (i) their morphology observed by phase contrast microscopy; (ii) ultrastructural analysis using transmission electron microscopy (TEM) analysis; (iii) CD marker expression, detected using immunostaining, reverse transcriptase-polymerase chain reaction (RT-PCR) and flow cytometry analysis; and (iv) differentiation ability using a commercial assay (osteogenic, adipogenic and chondrogenic differentiation assay). The differentiation potential of both cell types was compared using gene expression analysis techniques.

Materials and methods

rbMSC isolation

Rabbit bone marrow was harvested from New Zealand white rabbits with the protocol approved by the Animal Care and Use Committee, Faculty of Medicine, University of Malaya (PM/24/06/2008/TKZ). Three adult New Zealand white rabbits (at least 4 months old) were killed by an overdose of pentobarbital sodium (Nebutal® Sodium Solution; Boehringer, Ingelheim, Germany). Rabbit bone marrow was isolated from the tibial and femoral bones, and resuspended in 2 mL of phosphate-buffered saline (PBS; pH 7.2; Invitrogen-Gibco, USA). The bone marrow suspension was layered on 3 mL Ficoll-Paque™ Premium (density: 1.077 g mL^{-1}; GE Healthcare, Sweden) for gradient centrifugation at 400 g for 30 min in a 15-mL centrifuge tube.

The mononuclear layer (second top layer) was collected and then washed twice using Dulbecco's modified Eagle's medium (DMEM)-low glucose (DMEM-LG; 1000 mg L^{-1} D-Glucose; Invitrogen-Gibco) supplemented with antibiotic/antimycotic 1% (v/v; Invitrogen-Gibco). Next, the isolated mononuclear cells were cultured in growth medium [DMEM-LG (Invitrogen-Gibco) supplemented with 10% foetal bovine serum (Invitrogen-Gibco), antibiotic/antimycotic (Invitrogen-Gibco) 1% (v/v) and 200 mM GlutaMAX™-I (Invitrogen-Gibco)] in T75 tissue culture flasks (Nunc™, USA). The medium was changed at day 5 after primary culture to remove the non-adherent cells. The subsequent medium change was conducted at 3-day intervals. For comparison, human bone marrow was harvested from three adult donors (Table S1) undergoing intramedullary nailing of the femur or tibia in the University of Malaya Medical Center, and used for comparison with rbMSCs in the downstream experiments. hMSCs were isolated and expanded *in vitro* as previously described (Tan et al. 2012). Ethics approval to conduct this study was granted by the University of Malaya Medical Center Ethics Committee (reference no. 602.22).

Measurement of cell lengths and widths

Photographs were taken at representative areas of culture plates. The length and the maximum widths (cell body width) perpendicular to the long axes of individual cells were measured using ImageJ 1.46r software (National Institute of Mental Health, Maryland, USA). At least eight representative cells were measured from each independent experiment. Data were presented as mean ± standard error of mean. The statistical analysis was performed using SPSS Statistic software (version 19). Student's *t*-test (two-sided, unpaired)

was carried out to compare the differences in mean values, and a *P*-value < 0.05 was taken as significant.

rbMSC characterization by ultrastructural analysis

For electron microscopy, the medium was discarded from the culture flask containing rbMSC (or hMSC) at 70–80% confluence. The cells were rinsed twice with PBS (pH 7.2) (Invitrogen-Gibco) before being trypsinized and scraped from the flask with a cell scraper, centrifuged at 800 *g* for 10 min to form a cell pellet at the bottom of the centrifuge tube. The cell pellet was then fixed in 4% glutaraldehyde overnight before being further processed. The pellet was washed three times in 0.1 M cacodylate buffer (pH 7.4; Merck AG, Darmstadt, Germany),[i] prior to, and post-secondary fixation for 2 h at room temperature in a mixture of osmium tetraoxide : cacodylate buffer (1 : 1). The pellet was kept overnight in 0.1 M cacodylate buffer (pH 7.4; Merck AG). The next day, the pellet was washed with uranyl acetate for 10 min, followed by three washes with double-distilled water. Then, the pellet was dehydrated through a graded ethanol series (35, 50, 70 and 95%) for 10 min each; 100% for 15 min, three times; propylene oxide and epoxy resin mixture (1 : 0 for 15 min twice; 1 : 1 for 1 h; and 1 : 3 for 2 h), and in fresh epoxy resin, overnight, on the rotary mixer (Ted Pella, Redding, CA, USA), at 0.2 g. The specimen was then embedded in epoxy resin for semithin and ultrathin sectioning with an ultramicrotome (Reichert Ultracuts; Leica Microsystems, Vienna, Austria). Images were obtained with a TEM (Leo Libra 120; Carl Zeiss SMT AG, Oberkochen, Germany). Electron micrographs were prepared by the Electron Microscope Unit in University of Malaya.

rbMSC characterization by immunocytochemistry staining

Rabbit MSCs at P1 or P2 were seeded on a coverslip and used for CD44 immunocytochemistry staining. Briefly, the rbMSC cells were washed twice with cold PBS. Two-hundred microlitres of diluted (dilution at 1 : 1000) mouse mAb against rabbit CD44 surface antigen (Chemicon® International, Germany) used for staining was applied on to the cells and incubated in a humid chamber for 30 min. The cells were then washed again, twice, with cold PBS. Subsequently, the cells were stained with anti-mouse IgG allophycocyanin-conjugated Goat F $(ab')_2$ and counterstained with nucleus stain before mounting. Fluorescence images were captured using NIKON-ECLIPSE-TI-U microscope (Nikon, Japan) and NIS-ELEMENT AR software (Nikon).

rbMSC characterization by RT-PCR

Total RNA was extracted from 1×10^6 cells of 70–80% confluent rbMSC primary culture (P1–P3) using AllPrep DNA/RNA/Protein Mini kit[g] according to manufacturer's instructions and treated with RNase-free DNase I (Qiagen GmbH, Hilden, Germany). The gene-specific primers for RT-PCR were designed according to the mRNA sequence obtained from CD29 of *Felis catus* (GenBank accession FCU27351), and CD166, CD45 and CD34 of *Oryctolagus cuniculus* (GenBank accession Y13243, XM_002717662 and XM_002717543, respectively) using the *Primer Premier v5.0* (Table 1). The RT-PCR reactions were carried out using Superscript™ III One-Step RT-PCR System with Platinum^R Taq DNA Polymerase kit (Invitrogen, Carlsbad, CA, USA). The RT-PCR reactions were prepared according to the manufacturer's instructions (with some modifications) in a final volume of 25 μL with 12.5 μL 2 × reaction mix, 1 μL (or 1 μg) of total RNA, 10 μM of each primer, 1 μL of Superscript™ III RT/Platinum^R Taq Mix. The RT step involved incubation at 42 °C for 60 min. The amplification protocol was as follows: an initial denaturation of 94 °C for 2 min followed by 35 cycles of 94 °C for 15 s, 58 °C for 30 s and 72 °C for 30 s. Negative control tubes for each gene that contained water instead of template RNA or cDNA were also run under the same conditions. Glyceraldehyde-3-phosphate dehydrogenase (GAPDH) was used as internal control and RNA from mononuclear cells was used as positive control. To confirm the absence of primer-dimers and other spurious products, the PCR products were evaluated using an Experion™ automated microfluidic electrophoresis system (BioRad) as described in the manufacturer's protocol. This provides high-resolution banding patterns of the separated DNA molecules as well as the quantitative output of their relative abundance. Briefly, a small aliquot (~1 μL) of PCR product or DNA ladder was loaded into the sample well or ladder well on the DNA 1 K chip

Table 1 Primers used for RT-PCR and qPCR analysis.

Gene	Forward primer sequence	Reverse primer sequence	Amplicon size (bp)	GenBank accession no
RT-PCR				
CD29	5′-CAAGAAGGAATGCCTACGTC-3′	5′-CAATGCCACCAAGTTTCCCAT-3′	720	FCU27351
CD166	5′-GCTCCCCAGTATTTATTGCCTTC-3′	5′-GTAGCACCT TTCCATTCCTGTA-3′	345	Y13243
CD45	5′-AGGTAGTAGATGTTTTCCAAGTAGTGA-3′	5′-ACTTGTCCATTCTGGGCAGGGTAG-3′	130	XM_002717662
CD34	5′-AGAACTTTCCAGCATGTTCCAGTTTATG-3′	5′-GGCTTGCCACATCTTGCTCGGTGA-3′	95	XM_002717543
qPCR				
Col-I	5′-CTGACTGGAAGAGCGGAGAG-3′	5′-TCTGGGCAATGCTGGGCTGTGTGGG-3′	129	AY633663 (Tan et al. 2012)
Scx	5′-CAG CGG CAC ACG GCG AAC -3′	5′-CGT TGC CCA GGT GCG AGA TG -3′	165	BK000280 (Kuo & Tuan, 2008)
Ppar–γ	5′-AGCAAAGAAGTCGCCATCC-3′	5′-CGTTCAAGTCAAGGCTCACA-3′	118	NM_001082148
Runx2	5′-TCAGGCATGTCCCTCGGTAT-3′	5′-TGGCAGGTAGGTATGGTAGTGG-3′	54	AY598934
Sox9	5′-AGAGCGAAGAGGACAAGTTCCCCGT-3′	5′-ATGGGCACCAGCGTCCAGTCGTAG C-3′	85	XM_002719499
RT-PCR and qPCR				
GAPDH	5′-AACATCATCCCTGCCTCTACTG-3′	5′-CTCCGACGCCTGCTTCAC-3′	196	NM_002046 (Kuo & Tuan, 2008)

Table 2 Fluorescence-conjugated monoclonal antibodies used for immunophenotyping of rbMSC and hMSC.

Antigens	Fluorochrome-conjugate	Manufacturer	Applications
CD29	Non-conjugated	Abcam, UK	Rabbit only
CD29	APC	BD Biosciences, USA	Human only
CD44	Non-conjugated	SeroTec, USA	Rabbit only
CD44	APC	BD Biosciences, USA	Human only
CD73	PE-Cy™ 7	eBioscience, CA, USA	Rabbit only
CD73	PE-Cy™7	BD Biosciences, USA	Human only
CD73	FITC	BD Biosciences, USA	Human only
CD81	APC	BD Biosciences, USA	Rabbit and Human
CD90	PE-Cy™ 7	BD Biosciences, USA	Rabbit and Human
CD34	PerCP-Cy5.5	Santa Cruz Biotechnology, CA, USA	Rabbit only
CD34	PE	BD Biosciences, USA	Human only
CD34	PerCP-Cy5.5	BD Biosciences, USA	Human only
CD45	Non-conjugated	Gentaur Molecular Products, Belgium	Rabbit only
CD45	APC-H7	BD Biosciences, USA	Human only
CD117	PE	BD Biosciences, USA	Rabbit and Human
HLA-DR	FITC	BD Biosciences, USA	Rabbit and Human

(Bio-Rad, Hercules, CA, USA) and analysed with the Experion™ automated electrophoresis system (Bio-Rad). An electropherogram and a virtual gel were generated by the Experion software analysis tool when the run was completed for each sample, and the sizing of the PCR product was performed automatically based on the DNA standard electropherogram.

Flow cytometry analysis

Both rbMSCs and hMSCs at P2 or P3 were trypsinized at 70–80% confluence for phenotypic characterization using fluorescence-activated cell sorting (BD FACS Cantor II, BD Biosciences, USA). The cells were resuspended in PBS (pH 7.2) at a concentration of 10^7 cells mL^{-1}. A 100-μL cell suspension was transferred into each 5-mL polystyrene round-bottomed tube for incubation on ice with the optimum dilution of fluorochrome-conjugated mAbs or tandem dye-conjugated mAbs (Table 2). Alternatively, the cells were preincubated with non-conjugated mAbs followed by a secondary rat anti-mouse IgG–FITC or IgG–PE or IgG–APC and the fluorescence-conjugated mAb, at 4 °C for 30 min. The MSC-positive antigens included in the phenotyping profile were: CD29, CD44, CD73, CD81 and CD90.1. To discriminate MSCs from haematopoietic stem and progenitor cells, isolates were stained for CD34, CD45, CD117 and HLA-DR. All mAbs were immunoglobulin G_1 (IgG_1) isotype except for HLA-DR, which is immunoglobulin G_{2b} (IgG_{2b}). After 30 min of incubation, cells were washed using 2 mL PBS. Non-specific fluorescence emission was detected by incubating cells with fluorescence-conjugated isotype control. At least 10 000 events were captured by the system. Flow cytometry data were analysed using CELLQUEST software (Becton Dickinson). Gating was performed to exclude cell debris and unwanted aggregates (FSC/SSC dotplot). Non-specific isotype control (IgG_1 or IgG_{2a}) was used to determine the background fluorescence emission, if any.

AlamarBlue® cell proliferation assay

Cell proliferation was assessed using the alamarBlue® assay based on the colorimetric quantitative analytical principle. Both rbMSCs and hMSCs (at P2 or P3, $n = 3$) were seeded in standard 96-well culture plates at a cell density of 7.5×10^4 cells mL^{-1} in 250 μL of cell culture medium. Cells were incubated for 4 h before 25 μL of alamarBlue® reagent (Invitrogen-Gibco) was added into the medium. Culture plates were protected from light using aluminium foil. Absorbance readings at 570 and 600 nm were obtained using a spectrophotometer (Epoch; Biotek, USA) at various time points, i.e. at 0, 2, 4, 6, 12, 24, 36, 48, 60, 72, 84 and 96 h. Three independent experiments were performed, each in quadruplicate using 96-well plates. As a negative control, alamarBlue® reagent was added into the medium without cells. Data were presented as the mean ± standard deviation. Statistical analysis was analysed with SPSS (version 17) software. Comparisons of mean values between rbMSCs and hMSCs at various time points were conducted using Mann–Whitney *U*-test. Statistical significance was accepted at $P < 0.05$.

rbMSC differentiation assay

To further elucidate that the isolated rbMSCs have multi-lineage differentiation potential, rbMSCs were differentiated into tri-lineages (osteogenic, adipogenic and chondrogenic lineages) using the standard induction media. Osteogenic and adipogenic differentiation of rbMSCs was accomplished using commercially available standard differentiation induction media, namely STEMPRO® osteogenesis differentiation kit and STEMPRO® adipogenesis differentiation kit (Invitrogen-Gibco) in accordance with the manufacturer's protocol. Chondrogenic differentiation of rbMSCs was accomplished by using a modified protocol outlined by Mackay et al. (1998). The chondrogenic medium was prepared to that which was previously described (Tan et al. 2011). Cells were trypsinized, washed using PBS (pH 7.2; Invitrogen-Gibco) and then seeded in serum-free chondrogenic medium as previously described (Tan et al. 2011). The medium was changed at 3-day intervals. Differentiation potential was assessed by histological staining, i.e. Von Kossa staining for osteogenic differentiation; oil-red-O staining for adipogenic differentiation and safranin-O staining for chondrogenic differentiation; at day 28 of differentiation induction.

For gene expression analysis, cells were trypsinized at day 7 and day 28, and used for total RNA isolation. Quantitative RT-PCR (qPCR) was conducted as previously described (Tan et al. 2011).

Results

rbMSC isolation and culture

Isolation of rbMSCs was achieved by using the Ficoll-Paque gradient centrifugation. This technique stratified the MSC-like populations cells into a single layer, which allowed us to extract a high concentration of MSCs more effectively (Neagu et al. 2005). To aid the selection of rbMSC only,

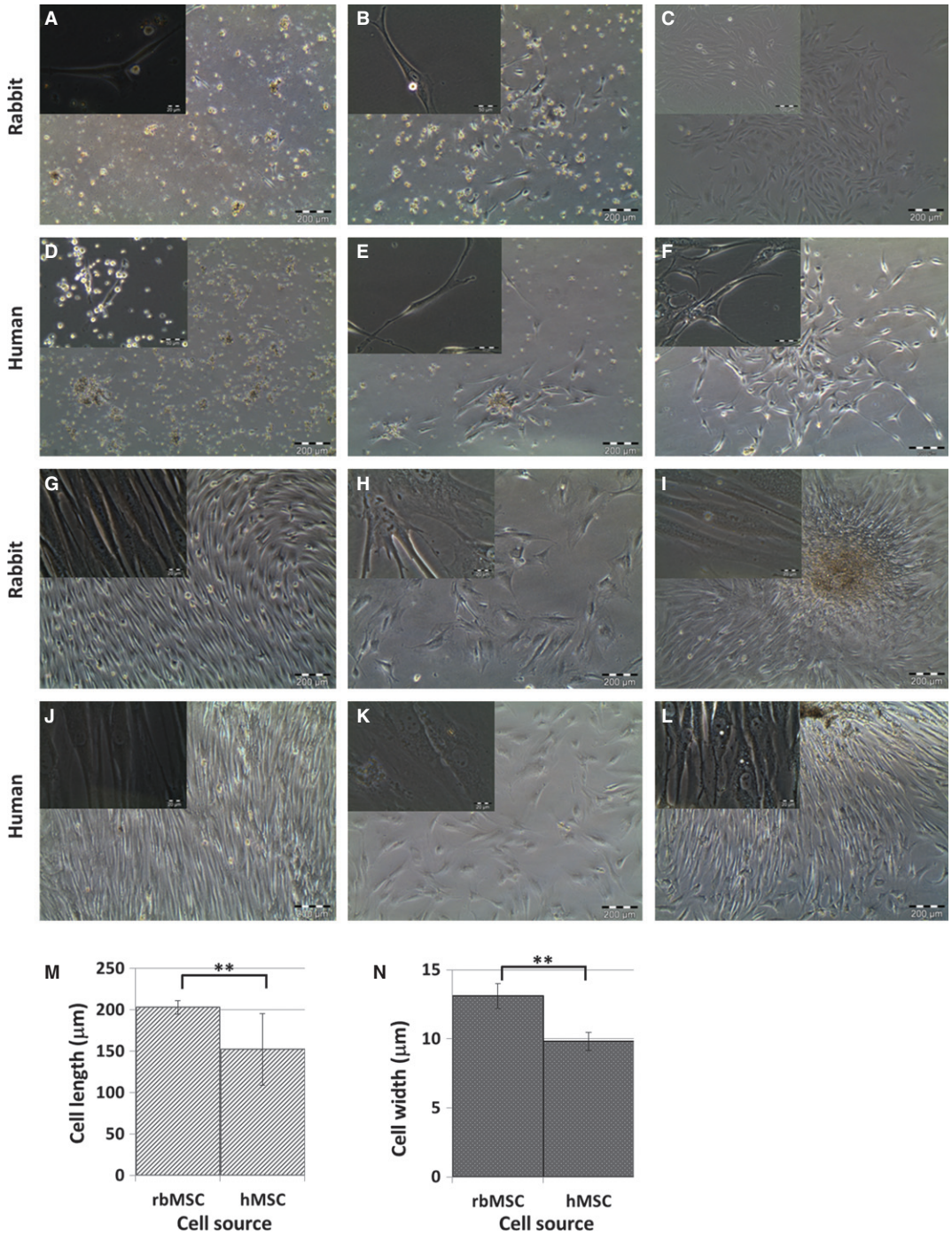

Fig. 1 Morphology of primary culture of rabbit and human bone marrow-derived mesenchymal stem cells (rbMSC and hMSC, respectively) observed under phase contrast microscope at 4 × objective (images of 40 × objectives were shown on the left upper corner of each image). Representative images from three independently performed experiments were shown (A–L). The cell length and width of eight representative cells from each individual experiment ($n = 3$) were measured and data are presented as mean ± standard error of the mean (M, N). Cells were fibroblastic spindle-shaped at days 4, 7, 10 and 24 in rbMSC cultures (A, B, C and G, respectively), and in hMSCs cultures (D, E, F and J, respectively). Some non-fibroblastic flat cells were observed in rbMSC (H) cultures and hMSC cultures (K) upon sub-culturing (P1 onwards). The majority of the cells remained fibroblastic spindle-shaped in rbMSCs (I) and hMSCs (L) upon sub-culturing from P1 to P3. The rbMSCs possessed significantly higher cell length (M) and cell width (N) compared with hMSCs ($P < 0.05$).

harvested cells were then seeded onto plastic cell culture flasks. Only those that adhered to the flask surfaces were maintained (Fig. 1A,B). After at least four medium changes over a period of 8–12 days, which resulted in the removal of the majority if not all non-adherent cells (Fig. 1C), the remaining cells appeared to have heterogeneous fibroblas-

tic-like appearance and formed distinct colonies on flask surfaces (Fig. 1C). This cell type appeared to form the majority of the cell population observed in cultures thereafter (Fig. 1G). These observations were similar to that of hMCS cultures (Fig. 1D–G). In the subsequent passages, i.e. P1 to P3, cultures with low proliferative (prolonged passage time), large polygonal and flattened cells with short or no processes (Fig. 1H,K) were discarded. The rbMSC-like cultures demonstrated increased proliferation, gradually and uniformly maintaining a homogeneous fibroblastic morphology. Cells from both rbMSCs and hMSCs were mainly of spindle-shaped appearance and elongated morphology with two processes that extended in opposite directions from a small cell body (Fig. 1B,E). These appearances were consistent and similar in both rbMSCs and hMSCs, with both cells not demonstrating any particular distinctive features that can conclusively define one from the other. Although cells appeared to be stretched with long and thin processes, these cells tended to group in close contact, parallel arrangement and grow in high-density colonies (Fig. 1I,L).

Table 3 A summary of similarities and differences between rbMSCs and hMSCs.

	Characteristics	rbMSC	hMSC
1	Isolation method	Gradient centrifugation using Ficoll-Paque™ Premium (density: 1.077 g mL^{-1})	
2	Plastic adherence	Yes	
3	Morphology	Fibroblastic spindle-shaped with two processes that extended in opposite directions from the cell body and grow in high-density colonies	
4	Ultrastructural characteristic	A large eccentric and irregular-shaped nucleus with a prominent nucleolus. Chromatin formed a thin and dense layer inside the perinuclear cisternae A rich inner cytoplasmic zone A small amount of Golgi rough endoplasmic reticulum, mitochondria and polyribosome The periphery of the plasma membrane displayed many small pseudopodia	
5	Cell size (μm)	Length: 202.66 ± 8.4 Width: 13.09 ± 0.91	Length: 152.04 ± 43.35 Width: 9.82 ± 0.66
6	Proliferation rate	Significantly lower than hMSC before 48 h Population doubling: 6.4 ± 1.3 h	Significantly higher than rbMSC after 48 h Population doubling: 7.6 ± 1.7 h
7	Phenotypic expression	Highly expressed: CD29, CD44, CD73, CD81 and CD90 Low expression: CD117, CD45 Negative expression: CD34 and HLA-DR	Highly expressed: CD29, CD44, CD73, CD81 and CD90 Negative expression: CD34, CD45, CD117 and HLA-DR
8	Differentiation conditions	StemPro® osteogenesis differentiation medium for osteogenic differentiation induction StemPro® adipogenesis differentiation medium for adipogenic differentiation induction Chondrogenic medium was prepared according to protocol outlined by Mackay et al. (1998)	
9	Differentiation potential (histological observation)	Osteogenic differentiation: Revealed by Von Kossa staining, which showed intracellular deposition of calcium oxalate crystals Adipogenic differentiation: Revealed by oil-red-O staining with presence of intracellular lipid droplets Chondrogenic differentiation: Revealed by safranin-O staining with presence of apparent glycosaminoglycans or highly sulphated proteoglycans	
10	Differentiation potential (gene expression)	Upregulation of osteogenic marker (*Runx2*) at days 7 and 28, upon osteogenic differentiation induction. Higher *Runx2* expression was observed in rbMSCs compared with hMSCs Upregulation of adipogenic marker (*Pparγ*) at day 28, upon adipogenic differentiation induction. No significant difference in *Pparγ* expression between rbMSCs and hMSCs Upregulation of chondrogenic marker (*Sox9*) at days 7 and 28, upon chondrogenic differentiation induction. Higher *Sox9* expression was observed in rbMSC compared with hMSCs	Upregulation of *RUNX2* at day 28, upon osteogenic differentiation induction Upregulation of *PPARγ* at day 28, upon adipogenic differentiation induction Upregulation of *SOX9* at days 7 and 28, upon chondrogenic differentiation induction

hMSC, human mesenchymal stem cell; rbMSC, rabbit mesenchymal stem cell.

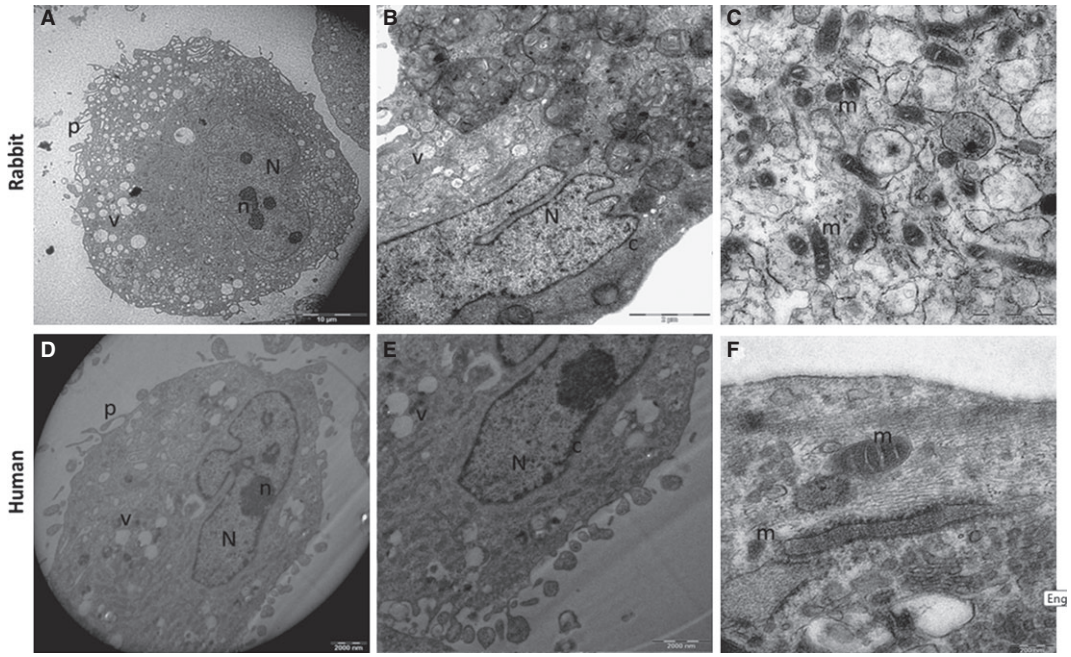

Fig. 2 TEM analysis of the ultrastructure of rbMSCs and hMSCs. Representative images of rbMSCs and hMSCs ultrastructure were shown. Both rbMSCs and hMSCs showed similar ultrastructure features. An eccentric and irregular-shaped nucleus (N), usually with multiple nucleoli (n), with various mitochondrial profiles (m), and small vacuoles (v) in rbMSCs (A, B) and hMSCs (D, E). Chromatin formed a thin and dense layer inside the perinuclear cisternae (c), and the plasma membrane formed many thin pseudopodia (p). Mitochondria showed both a rounded and elongated profile with thick cristae in both rbMSCs (C) and hMSCs (F).

However, there were cells that were widely dispersed; most of these cells formed colonies eventually. A summary of the description and similarities between these cells is presented in Table 3. These rbMSC-like cells were maintained and subcultured up to P3 for downstream analysis.

Although similar in their morphological appearance, the rbMSCs cell length ($202.66 \pm 8.40\ \mu m$) and width ($13.09 \pm 0.91\ \mu m$) were significantly longer and wider than hMSCs ($152.04 \pm 43.35\ \mu m$ in length; $9.82 \pm 0.66\ \mu m$ in width; $P < 0.01$; Fig. 1M,N).

rbMSC ultrastructural analysis

In the ultrastructural analysis, rbMSCs displayed phenotypic appearances that were indistinguishable from hMSCs (Fig. 2). They were relatively uniform in their ultrastructural characteristics. Generally, both rbMSCs and hMSCs possessed a large, eccentric, irregular-shaped nucleus and a rich inner cytoplasmic zone (Fig. 2A,B,D,E). The nucleus showed multiple nucleoli, and the chromatin formed a thin and dense layer inside the perinuclear cisternae. The periphery of the plasma membrane displayed many small pseudopodia in both rbMSCs and hMSCs (Fig. 2A,D). In addition, within the rich cytoplasm region (Fig. 2A,B), a small amount of Golgi rough endoplasmic reticulum as well as a modest number of mitochondrial with different profiles (rounded and elongated profile with thick cristae) were present. There was neither fat globules in the cells nor ultrastructural disruption, denoting that no cells were at the senescence stage of development.

rbMSC surface markers expression

Immunofluorescence staining to detect CD44 surface markers was positive for rbMSCs (Fig. 3A). RT-PCR analysis demonstrated a positive expression for CD29 and CD166 in rbMSCs (Fig. 3B), but was negative for other surface markers (CD45 and CD34; Fig. 3B). GAPDH was used as the housekeeping gene, whilst positive and negative controls were also performed for the surface protein markers: CD29, CD166, CD45 and CD34 (data not shown).

Flow cytometry analysis

Based on the mAbs available for rbMSC, this study elucidates that rbMSCs express multiple markers of MSCs. The cultured rbMSCs revealed positive for CD29, CD44, CD73, CD81 and CD90, but were negative (or dim positive) for CD34, CD45, CD117 and HLA-DR (Table 4A). In the multi-colour, at least 70% of rbMSCs expressed double-positive expression, double-negative or co-expressed positive and negative markers as compared with 90% of that in hMSCs. These analyses are summarized in Table 4B.

Important note: there were no other markers that were tested on these cells that yielded negative or positive results

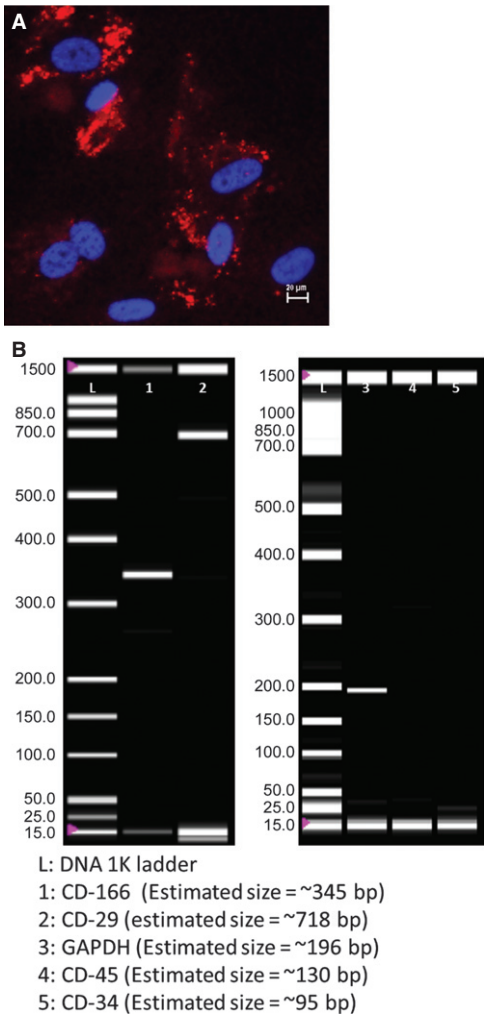

Fig. 3 Immunofluorescence staining image for positive expression of CD44 [in red, anti-mouse IgG allophycocyanin-conjugated goat F $(ab')_2$] counterstained with nucleus stain (in blue) in both rbMSC and hMSC. (B) RT-PCR analysis for CD166 (lane 1), CD29 (lane 2), CD45 (lane 4), CD34 (lane 5) and GAPDH (in lane 3). Lane L indicates the DNA ladder. The presence of amplicon in lanes 1–3 indicated positive expression of the corresponding genes, and the absence of amplicon in lanes 4 and 5 denoted that these genes were not expressed.

in both the flow cytometry and immunohistochemistry analyses.

AlamarBlue® cell proliferation assay

The results of alamarBlue® assay showed a growth curve of rbMSC and hMSC, both appearing as a typical 'S-shaped curve' seen in many cell cultures (Fig. 4). No significant differences were observed in the alamarBlue® reduction in both rbMSCs and hMSCs during the 'lag phase' of cell proliferation. However, as the cells enter into their exponential 'log phase', rbMSCs showed significantly lower ($P < 0.05$) cell proliferation than hMSCs, at 48 h during the cell culture. The rbMSCs reached a plateau phase at 72 h, as compared with 48 h in hMSCs. The population doubling times of rbMSCs and hMSCs were 6.4 ± 1.3 and 7.6 ± 1.7 h, respectively. However, there were no significant differences between the two ($P > 0.05$).

rbMSC tri-lineage differentiation assay

Using the osteogenic differentiation assay, the presence of calcium oxalates was clearly observed from the Von Kossa staining on the differentiated rbMSCs, which was not present in the undifferentiated cells (Fig. 5A). The use of safranin-O aided the detection of proteoglycan deposition in chondrogenic-induced rbMSCs; however, this was negative in the control group (Fig. 5B). Adipogenesis of rbMSCs was detected by staining intracellular lipid droplets using oil-red-O (Fig. 5C) in the adipogenic-induced rbMSC cultures. This was also absent in the undifferentiated rbMSCs. These observations suggest that rbMSCs have the potential to undergo the tri-lineage, i.e. osteogenic, chondrogenic and adipogenic, differentiation required to fulfill the characteristics of MSCs. As compared with cultured hMSCs, these cells appear to have similar characteristics.

Gene expression quantification analysis of rbMSC tri-lineage differentiation potential

rbMSCs expressed significantly higher *Runx2* (osteogenic marker) and *Sox9* (chondrogenic marker) expression on both day 7 and day 28 as compared with that of hMSC ($P < 0.05$). In adipogenic medium, both rbMSCs and hMSCs showed similarly elevated *Ppar*γ (adipogenic marker) gene expression levels on day 28 ($P > 0.05$; Fig. 6). A summary of gene expression levels in rbMSC tri-lineage differentiation potential as compared with hMSCs is described in Table 3.

Discussion

The present study demonstrates that similar techniques used to isolate hMSCs may be used to isolate rbMSCs. We identified that rbMSCs possess characteristics similar to those of hMSCs based on the following findings: (i) the rbMSCs were adherent to plastic and demonstrated fibroblastic spindle shape with two processes that extended in opposite directions from the cell body as observed under phase contract microscope (Fig. 1B); (ii) the ultrastructural characteristics and morphology observed using TEM were similar to that of hMSCs; (iii) the specific antigens expression in rbMSCs identified using immunohistology staining, RT-PCR and flow cytometry were similar to that defined in hMSC, i.e. $CD29^+$, $CD44^+$, $CD73^+$, $CD81^+$, $CD90^+$, $CD166^+$, $CD34^-$ (dim), $CD45^-$ (dim), $CD117^-$ (dim) and HLA-DR^- expression; and (iv) histology staining (Von Kossa, safranin-O and staining oil-red-O) indicates that rbMSCs are able to undergo tri-lineage differentiation when cultured using the appropriate differentiation medium for osteogenic,

Table 4 Summary of flow cytometry analysis for (A) single marker and (B) co-expression of two markers.

A

Cell type	$CD29^+$ (%)	$CD44^+$ (%)	$CD73^+$ (%)*	$CD81^+$ (%)	$CD90^+$ (%)*	$CD34^+$ (%)*	$CD45^+$ (%)*	$CD117^+$ (%)	$HLA\text{-}DR^+$ (%)*
rbMSC	85.0	81.6	96.4	96.9	96.9	7.1	18.0	17.4	4.3
hMSC	100.0	99.6	98.6	99.9	100.0	0.2	0.1	1.4	0.2

B

Antigens	rbMSC (%)	hMSC (%)
$CD29^+$ and $CD34^-$*	78.4	99.8
$CD44^+$ and $CD73^+$*	70.9	93.7
$CD44^+$ and $CD34^-$*	82.1	98.4
$CD90^+$* and $CD73^+$*	70.1	96.4
$CD90^+$* and $CD81^+$	89.8	100.0
$CD90^+$* and $CD34^-$*	89.8	97.3
$CD90^+$* and $CD45^-$*	81.6	92.0
$CD90^+$* and $CD117^-$	79.6	99.0
$CD73^+$* and $CD81^+$	75.0	99.5
$CD73^+$* and $CD34^-$*	83.2	97.7
$CD73^+$* and $CD117^-$	71.2	98.6
$CD81^+$ and $CD34^-$*	91.8	98.0
$CD81^+$ and $CD117^-$	76.9	98.6
$CD81^+$ and $HLA\text{-}DR^-$*	76.3	99.4
$CD34^-$* and $CD45^-$*	76.2	91.0
$CD34^-$* and $CD117^-$	77.3	97.0
$CD45^-$* and $HLA\text{-}DR^-$*	72.0	97.7

MSC-positive antigens (+): CD29 (Integrin β1), CD44 (H-CAM, PGP-1), CD73 (Ecto-5′-nucleotidase, NT5E), CD81 (TAPA-I) and CD90 (Thy-1). MSC-negative antigens (−): CD34. CD45 (leukocyte common antigen, Ly-5), CD117 (SCF R, c-Kit) and HLA-DR (MHC Class-II).
*CD markers that are prerequisite by ISCT criteria.
hMSC, human mesenchymal stem cell; rbMSC, rabbit mesenchymal stem cell.

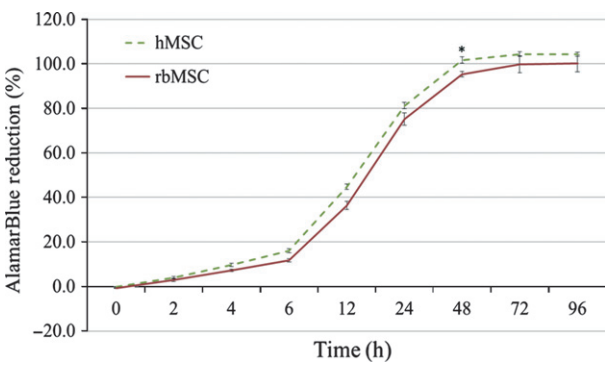

Fig. 4 AlamarBlue® cell proliferation assay of rabbit mesenchymal stem cells (rbMSCs) and human (h)MSCs cultures. There were no significant differences in cell proliferation rates at the lag phase and plateau phase, but the hMSCs showed significantly higher alamarBlue® reduction at the log phase, after 48 h ($P < 0.05$).

adipogenic and chondrogenic differentiation. Nevertheless, there are differences that are worth mentioning. Our results demonstrate that between rbMSCs in hMSC: (i) the cell size of rbMSCs was significantly larger than hMSCs ($P < 0.05$); (ii) the cell proliferation of rbMSCs was lower than that of hMSCs ($P < 0.05$); and (iii) the *Runx2* (osteogenic marker) and *Sox9* (chondrogenic marker) gene expressions levels were significantly higher in rbMSCs at day 7 and 28 as compared with that of hMSC ($P < 0.05$). All the similarities and differences between rbMSCs and hMSCs were also summarized in Table 3.

Based on the current technique used to isolate rbMSCs, it appears that at P3, both rbMSCs and hMSCs produced sufficient cells for analyses, specifically for flow cytometry and qPCR, to be conducted successfully. However, the present study did not measure cell quantity in order to determine the yield potential of the technique used, as this was outside the scope of the study. Consistent with previous reports, fibroblastic rbMSCs cultured in this study tend to form cell colonies, arranged in parallel assembly, and grow in high-density colonies, similar to those observed in human (Castro-Malaspina et al. 1980), mouse (Friedenstein et al. 1982; Mori et al. 1987), rat (Fu et al. 2012) and rabbit (Owen et al. 1987) MSCs. The high-density colony characteristics were also similar to those observed in other matured cell types (Selvaratnam et al. 2005). In this study, the

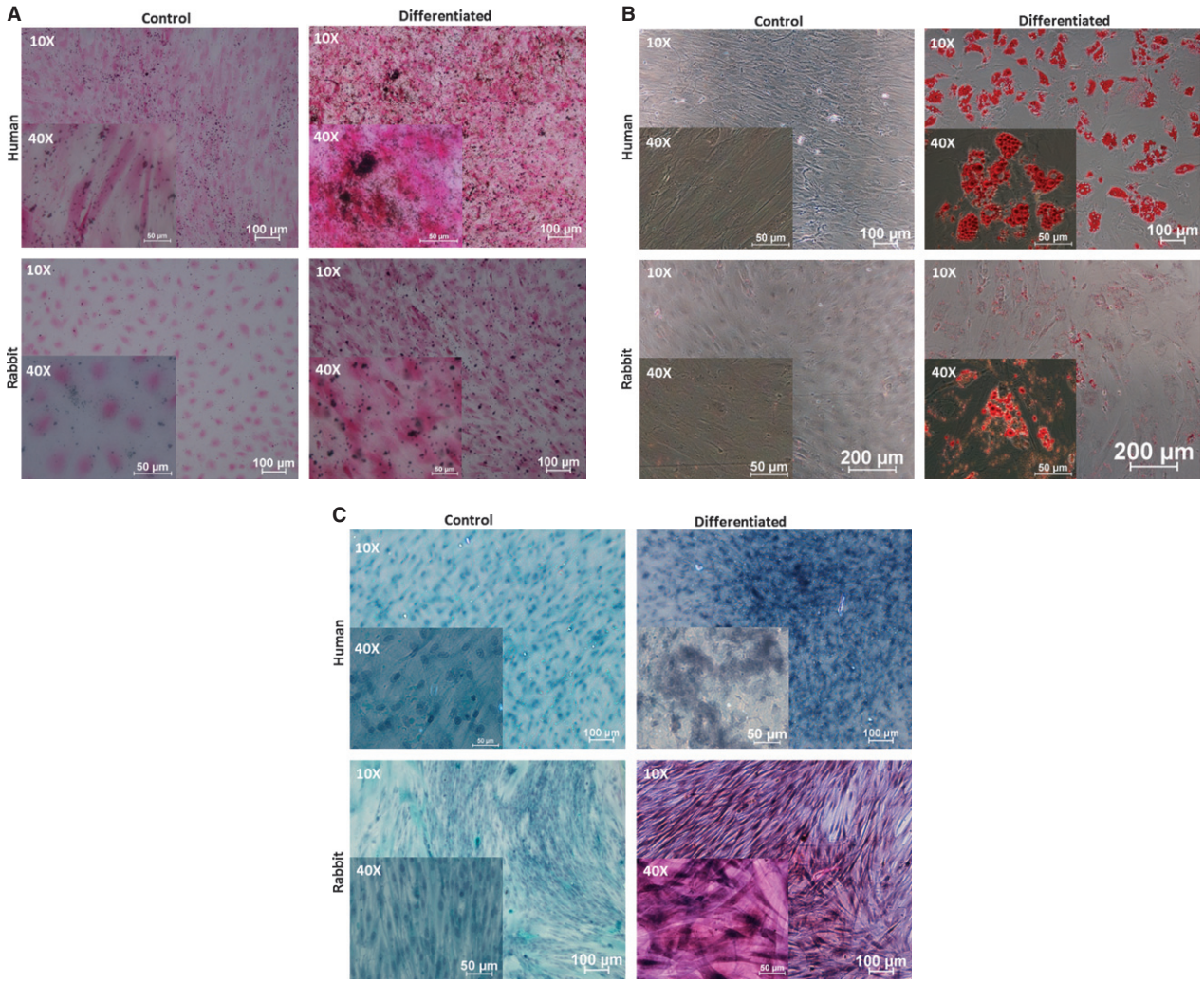

Fig. 5 Tri-lineage differentiations of primary rbMSCs. (A) Osteogenic differentiation of rbMSC and hMSC (as positive control) for 28 days. rbMSC and hMSC were cultured in standard MSC growth medium (control cultures) or osteogenic induction medium. Lower images: intracellular deposition of calcium oxalate crystals (black colour signifies) in osteogenic-rbMSCs as revealed by Von Kossa staining (right). No accumulation of calcium oxalate crystals was observed in uninduced control rbMSC culture stained with Von Kossa staining for comparison (left). Upper images: positive control of adipogenic differentiation in hMSCs (right) and non-induced control hMSC (left) stained with oil-red-O staining. Magnifications were denoted at the upper left corner of the images. (B) Adipogenic differentiation assay of rbMSC and hMSC (as positive control) for 28 days. rbMSC and hMSC were cultured in standard MSC growth medium (control cultures) or adipogenic induction medium. Lower images: presence of intracellular accumulated lipid droplets (red colour in the image) in adipogenic-rbMSCs as revealed by oil-red-O staining (right). No accumulation of lipid droplets was observed in non-induced control rbMSC culture stained with oil-red-O staining for comparison (left). Upper images: positive control of adipogenic differentiation in hMSCs (right) and uninduced control hMSC (left) stained with oil-red-O staining. Magnifications were denoted at the upper left corner of the images. (C) Chondrogenic differentiation assay of rbMSC and hMSC (as positive control) for 28 days. rbMSC and hMSC were cultured in standard MSC growth medium (control cultures) or chondrogenic induction medium. Lower images: presence of glycosaminoglycans or highly sulphated proteoglycans (pinkish colour in the image) in chondrogenic-rbMSCs as revealed by safranin-O staining (right). No accumulation of glycosaminoglycans was observed in non-induced rbMSC culture stained with safranin-O for comparison (left). Upper images: positive control of chondrogenic differentiation in hMSCs (right) and non-induced control hMSC (left) stained with safranin-O. Magnifications were denoted at the upper left corner of the images.

rbMSCs cultures that demonstrated large flat cells upon sub-culturing were discarded because the typical larger flat cellular morphology has been reported as: (i) senescent MSC (Cheng et al. 2003; Schellenberg et al. 2011; Fu et al. 2012); and (ii) associated with low proliferative rate and were less potential or characterized as 'mature' (Colter et al. 2000, 2001; Sekiya et al. 2002; Neuhuber et al. 2008). Besides, morphological heterogeneity has also been associated with different stages of cell differentiation rather than the existence of distinct cell types or subtypes (Sekiya et al. 2002; Smith et al. 2004; Docheva et al. 2008). This further alludes to the importance of culturing the subset of rbMSCs that is more homogeneous, proliferative and exhibits fibroblastic spindle-shaped for the downstream applications.

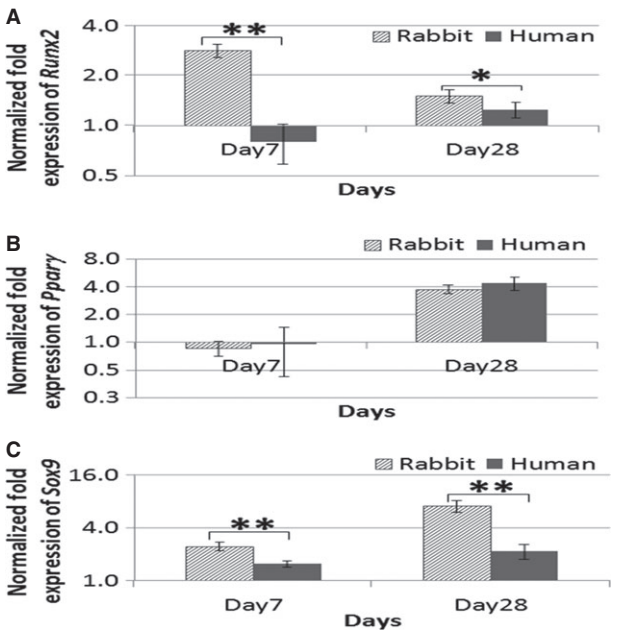

Fig. 6 Gene expression analysis of the cultured rbMSCs in the temporal experiment of tri-lineage differentiation assay, osteogenic (a), adipogenic (b) and chondrogenic (c) differentiation, at day 7 and day 28. The data reflected that the relative quantification of target mRNA normalized to control samples (untreated MSCs cultured in MSC growth medium). Data were presented as $\log_2$-fold change (with error bars signifying range of standard deviation). All the differentiation markers (*Runx2*, *Pparγ* and *Sox9*) were upregulated on day 28. However, spontaneous differentiation into osteogenic and chondrogenic lineages was observed in the rbMSCs with significant early upregulation of the respective differentiation markers (*Runx2* and *Sox9*) at day 7.

To determine the characteristics of rbMSC, electron microscopy has been an invaluable tool that has allowed us to make effective identification of rbMSCs based on the surface and internal morphological appearance that were similar to hMSCs. Our observations indicate that rbMSC and hMSC ultrastructures appeared similar to that previously reported in hMSC (Castro-Malaspina et al. 1980; Raimondo et al. 2006; Li et al. 2008). Raimondo et al. (2006) and Castro-Malaspina et al. (1980) described the hMSC as having a large, eccentric and irregular-shaped nucleus. In addition to the morphology of the nucleus, hMSC has been reported as being uni-nucleated (Raimondo et al. 2006), which was similar to that found in rbMSC. Similarly, mitochondria of various profiles (Raimondo et al. 2006; Li et al. 2008) and Golgi apparatus with typical stacks of flattened cisternae (Raimondo et al. 2006) were also observed in rbMSC (data not shown). The presence of pseudopodia surrounding the entire plasma membrane of rbMSCs has also been reported in rat MSC (Castro-Malaspina et al. 1980) and hMSC (Raimondo et al. 2006).

According to the ISCT guidelines (Dominici et al. 2006), one of the criteria that defines hMSC is phenotypic co-expression of CD105, CD90 and CD73 ($>95\%$), and lack of CD34, CD45, CD14, CD79 and HLA-DR ($<2\%$). Within the assessed hMSC donor cells, flow cytometry results showed that the cell culture populations consistently fulfilled all hMSC criteria (Table 3), including CD105, CD14 and CD19 (only tested in hMSCs; Supplementary #3). In comparison, the rbMSCs fulfilled the positive marker criteria set for hMSC (CD73 and CD90), but partly fulfilled the negative marker criteria set for hMSC (CD34, CD45 and HLA-DR) where dim expressions of the surface markers were observed for CD34 and CD45. A previous study demonstrated that bone marrow-derived MSCs in culture have a heterogeneous CD34 and CD45 phenotype that changes under *in vitro* conditions (Kaiser et al. 2007). This may explain the occurrence of $CD34^+$ and $CD45^+$ observed in rbMSCs. Whereas for the other CD markers evaluated, i.e. CD117 was also detected as dimly positive in rbMSCs (17.4%) whilst in hMSCs, this was negative (1.4%). On the contrary, CD81 was highly positive in rbMSCs (96.9%) as well as hMSCs (99.9%). CD29 and CD44 were also observed as being highly positive in rbMSCs (85% and 81.6%, respectively) and hMSCs (100 and 99.6%, respectively).

The expression of CD117 by MSCs is controversial. It has been previously reported in murine MSCs, and the expression levels have been demonstrated to decrease during extended serial passage (Meirelles LDA and NARDI, 2003). In isolated adipose tissue-derived stem cells, CD117 and HLA-DR expression have also been reported (Varma et al. 2007; Rebelatto et al. 2008). However, contrasting results have been reported in mouse MSC where negative expression of CD117 was observed (Nadri et al. 2007). This may be due to the loss of CD117 upon *in vitro* expansion (Meirelles LDA and NARDI, 2003). It is therefore logical to deduce that CD117 should be used as a potential marker of rbMSCs to determine if this expression would be lost in long-term cell cultures.

The rbMSCs are $CD44^+$ cells (Fig. 1B), similar to that previously reported in murine (Nadri et al. 2007) and canine (Seo et al. 2009) MSCs; and are $CD29^+$, which is consistent with that reported in rodent (Karaoz et al. 2009) and canine MSCs (Seo et al. 2009). Our findings also demonstrate that $CD166^+$ was present in rbMSCs, which is similar to that reported for human bone marrow- and cord blood-derived MSCs (Goodwin et al. 2001), and ovine bone marrow-derived MSCs (McCarty et al. 2009). Nevertheless, $CD166^+$ has been described as an inconsistent marker, as this protein gradually decreases over many passages in murine epiphysis-derived MSCs (Cheng et al. 2012). Whether this may be the case for rbMSCs remains to be elucidated, hence the loss of detection of this surface marker may not be enough to exclude the presence of rbMSCs.

The present study demonstrated that the cells obtained using the described method conformed to the criteria set by ISCT guidelines (Dominici et al. 2006), with the exception of several protein markers that are not available for testing. In this study, both qualitative and quantitative assays were used to determine the *in vitro* multi-lineage developmental potential of rbMSCs and hMSCs after *in vitro* exposure to

specific culture conditions. The hMSCs demonstrated a greater propensity to differentiate into the osteogenic and adipogenic lineages than rbMSCs based on the qualitative (histological staining) results. Induced hMSCs presented more prominent deposition of calcium oxalate crystals and more mature adipocytes (more lipid vacuoles present) than the induced rbMSCs under the same culture conditions. Only tiny amounts of calcium oxalate crystals or tiny lipid vacuoles were observed in rbMSCs after 28 days of induction. These observations suggest that differentiation occurs in rbMSC cultures but takes longer than hMSCs. In contrast, gene expression analysis demonstrates that rbMSCs express higher levels of osteogenic and chondrogenic marker gene expression by day 28. However, the adipogenic marker gene expression was similar to hMSC. The high expression of *Runx2* gene in rbMSC at day 7, but appears lower by day 28, may explain the observations of tiny calcium oxalate crystals on day 28 in rbMSCs. We can therefore suggest from the observation of this experiment, that the response of rbMSCs in osteogenic induction is more acute (by day 7) than hMSCs, but subsequently gradually decreases as it is kept in cultures longer. It may be the case that the regulation of adipogenic differentiation of rbMSCs is controlled at the protein translation level, and thus for the reason for not being able to observe large lipid vacuole despite having increased *Ppar*γ expression levels. Nevertheless, the higher *Sox9* expression levels in rbMSCs than hMSCs were consistent and appear to correspond to the increased intensity of the glycosaminoglycans observed from the safranin-O staining.

What is of interest in this study is that similar protocols and preparations used for hMSCs may be used for rbMSC differentiation without the need for any modification. This alludes to the fact that rbMSCs possess similar behaviour and capabilities as hMSCs, which is a strong point that supports the use of this cell in many studies. This is a quality that is especially important for translational research. However, there is a need to be cautious when interpreting the data of cellular differentiation as our study has demonstrated that rbMSCs appear to have the ability to express a higher level of osteogenic and chondrogenic gene expressions than that of hMSCs. Besides, the proliferation rate of rbMSCs was significantly lower than that of hMSCs. Because telomere length and telomerase activity are in relation to cell proliferation and aging, we postulated that hMSCs telomere length and telomerase activity are both greater than rbMSCs. Nevertheless, this speculation needs to be substantiated in further studies, which at the present time is not within the scope of current study.

With the results of the present study supporting our earlier hypothesis that rbMSCs can be isolated using established methods meant for hMSCs and that they possess similar characteristics to these cells, we propose that the set criteria that define hMSCs would be applicable to define rbMSCs, whilst using the present report as a reference. The criteria should include the plastic adherent behaviour, the described morphological appearances, selected CD markers expressed, and the ability to undergo tri-lineage differentiation. These criteria are summarized in Table 5.

Table 5 Summary of characteristics of rbMSC.

Minimum criteria to define rbMSC		
Adherent to plastic in standard culture conditions		
Fibroblastic spindle-shaped with two processes that extended in opposite directions from the cell body and grow in high-density colonies when cultured under standard culture conditions		
Phenotype (as revealed by flow cytometry analysis)	Positive CD29 CD44 CD73 CD81 CD90 CD117	Negative CD34 CD45 HLA-DR
Capable to undergo *in vitro* differentiation into osteogenic, chondrogenic and adipogenic lineages (as revealed by histological staining) when cultured in the appropriate differentiation medium		

rbMSC, rabbit mesenchymal stem cell.

Several unavoidable limitations were also identified. Firstly, isolation of rbMSCs was merely selected based on their plastic adherence characteristic. It would have been more accurate if antibody-specific approaches were utilized (Friedenstein et al. 1976; Taylor et al. 2007). Isolation and purification of rbMSCs using this method, however, was not available due to limited availability of mAbs for the rabbit model, particularly for those specific to MSCs surface molecules, i.e. CD105 (endoglin). In the future, it is hoped that these antibodies may become available (i.e. CD166 and CD105), thus producing more convincing results using more efficient isolation methods. Future study should also include CD166 (or other markers) in flow cytometry analysis once the mAb becomes available for rbMSCs. Secondly, not all the CD markers set to define hMSC were evaluated in rbMSCs, i.e. CD105, CD14 and CD19 (Dominici et al. 2006). This however, was hampered due to the scarcity in rabbit molecular biology information and limitations in the mAbs available for stem cell surface markers immunostaining. To overcome this problem, the use of gene expression analysis obtained by determining mRNA levels using gene-specific primers was an acceptable option for the present study. Custom-designed gene-specific primers for CD29, CD166, CD45 and CD34 based on their corresponding mRNA sequence information were designed from available information of *Oryctolagus cuniculus* or *Felis catus* or *Homo sapiens*. This was obtained from the NCBI GenBank database; and was helpful in defining the rbMSCs.

Conclusion

rbMSCs can be isolated using methods described previously for hMSCs. rbMSCs appear to have similar characteristics to that of hMSCs, and conform to most of the standards set by ISCT. Based on the results presented here and with reference to the ISCT guidelines (Dominici et al. 2006), we summarized that the minimum characteristics of rbMSCs in Table 5 should be used as a reference tool for future researchers, although we caution that revisions to the definitions or criteria should be made regularly as new data or new technologies emerge. Nevertheless, these criteria should suffice as the baseline that best identifies rbMSCs in view of the current state of knowledge. It is important to note that several differences between rbMSCs and hMSCs need to be acknowledged, for example proliferation, osteogenic/chondrogenic expressions, and that caution should be used when interpreting or translating data from rabbits to humans.

Acknowledgements

This study was supported by HIR-MOHE research grant initiative, eScience Grant (12-02-03-2017), UMRG (RG093/09HTM) and University of Malaya postgraduate student grant (PS167/2008C, PS360/2009B and PS219/2010A). We also thank the University of Malaya for a PhD thesis scholarship for the first author.

Conflict of interest

The authors indicate no potential conflicts of interest.

Authors' contribution

T.S.L. designed and performed experiments, acquired and analysed data as well as wrote the manuscript; L.S. supervised on data analysis/interpretation; T.S.A. and T.K.Z. supervised the experiment design, provided reagents and revised the manuscript critically; all authors were involved in final approval of the version to be submitted for reviewing/publication.

References

Amini AR, Laurencin CT, Nukavarapu SP (2012) Differential analysis of peripheral blood- and bone marrow-derived endothelial progenitor cells for enhanced vascularization in bone tissue engineering. *J Orthop Res* **30**, 1507–1515.

Bunnell BA, Flaat M, Gagliardi C, Patel B, Ripoll C (2008) Adipose-derived stem cells: isolation, expansion and differentiation. *Methods* **45**, 115–120.

Castro-Malaspina H, Gay RE, Resnick G, et al. (1980) Characterization of human bone marrow fibroblast colony-forming cells (CFU-F) and their progeny. *Blood* **56**, 289–301.

Chamberlain G, Fox J, Ashton B, Middleton J (2007) Concise review: mesenchymal stem cells: their phenotype, differentiation capacity, immunological features, and potential for homing. *Stem Cells* **25**, 2739–2749.

Cheng CC, Lian WS, Hsiao FS, et al. (2012) Isolation and characterization of novel murine epiphysis derived mesenchymal stem cells. *PLoS One* **7**, e36085.

Cheng L, Hammond H, Ye Z, Zhan X, Dravid G (2003) Human adult marrow cells support prolonged expansion of human embryonic stem cells in culture. *Stem Cells* **21**, 131–142.

Chong PP, Selvaratnam L, Abbas AA, Kamarul T (2011)Human peripheral blood derived mesenchymal stem cells demonstrate similar characteristics and chondrogenic differentiation potential to bone marrow derived mesenchymal stem cells. *J Orthop Res* **30**, 634–642.

Colter DC, Class R, Digirolamo CM, Prockop DJ (2000) Rapid expansion of recycling stem cells in cultures of plastic-adherent cells from human bone marrow. *Proc Natl Acad Sci USA* **97**, 3213–3218.

Colter DC, Sekiya I, Prockop DJ (2001) Identification of a subpopulation of rapidly self-renewing and multipotential adult stem cells in colonies of human marrow stromal cells. *Proc Natl Acad Sci USA* **98**, 7841–7845.

Dashtdar H, Rothan HA, Tay T, et al. (2011) A preliminary study comparing the use of allogenic chondrogenic predifferentiated and undifferentiated mesenchymal stem cells for the repair of full thickness articular cartilage defects in rabbits. *J Orthop Res* **29**, 1336–1342.

Docheva D, Padula D, Popov C, Mutschler W, Clausen-Schaumann H, Schieker M (2008) Researching into the cellular shape, volume and elasticity of mesenchymal stem cells, osteoblasts and osteosarcoma cells by atomic force microscopy. *J Cell Mol Med* **12**, 537–552.

Dominici M, Le Blanc K, Mueller I, et al. (2006) Minimal criteria for defining multipotent mesenchymal stromal cells. The International Society for Cellular Therapy position statement. *Cytotherapy* **8**, 315–317.

Fox RR (1984) The rabbit as a research subject. *The Physiologist* **27**, 393–402.

Friedenstein AJ, Gorskaja JF, Kulagina NN (1976) Fibroblast precursors in normal and irradiated mouse hematopoietic organs. *Exp Hematol* **4**, 267–274.

Friedenstein AJ, Latzinik NW, Grosheva AG, Gorskaya UF (1982) Marrow microenvironment transfer by heterotopic transplantation of freshly isolated and cultured cells in porous sponges. *Exp Hematol* **10**, 217–227.

Fu WL, Zhang JY, Fu X, et al. (2012) Comparative study of the biological characteristics of mesenchymal stem cells from bone marrow and peripheral blood of rats. *Tissue Eng Part A* **18**, 1793–1803.

Goodwin HS, Bicknese AR, Chien SN, Bogucki BD, Quinn CO, Wall DA (2001) Multilineage differentiation activity by cells isolated from umbilical cord blood: expression of bone, fat, and neural markers. *Biol Blood Marrow Transplant* **7**, 581–588.

Gupta R, Lee TQ (2007) Contributions of the different rabbit models to our understanding of rotator cuff pathology. *J Shoulder Elbow Surg* **16**, S149–S157.

Haasters F, Prall WC, Anz D, et al. (2009) Morphological and immunocytochemical characteristics indicate the yield of early progenitors and represent a quality control for human stem cell culturing. *J Anat* **214**, 759–767.

Kaiser S, Hackanson B, Follo M, et al. (2007) BM cells giving rise to MSC in culture have a heterogeneous CD34 and CD45 phenotype. *Cytotherapy* **9**, 439–450.

Karaoz E, Aksoy A, Ayhan S, Sariboyaci AE, Kaymaz F, Kasap M (2009) Characterization of mesenchymal stem cells from rat bone marrow: ultrastructural properties, differentiation potential and immunophenotypic markers. *Histochem Cell Biol* **132**, 533–546.

Koerner J, Nesic D, Romero JD, Brehm W, Mainil-Varlet P, Grogan SP (2006) Equine peripheral blood-derived progenitors in comparison to bone marrow-derived mesenchymal stem cells. *Stem Cells* **24**, 1613–1619.

Kuo CK, Tuan RS (2008) Mechanoactive tenogenic differentiation of human mesenchymal stem cells. *Tissue Eng Part A* **14**, 1615–1627.

Laitinen A, Laine J (2007)Isolation of mesenchymal stem cells from human cord blood. *Curr Protoc Stem Cell Biol* **1**, 2A.3.1–2A.3.7.

Li Y, Zhang C, Xiong F, et al. (2008) Comparative study of mesenchymal stem cells from C57BL/10 and mdx mice. *BMC Cell Biol* **9**, 24.

Mackay AM, Beck SC, Murphy JM, Barry FP, Chichester CO, Pittenger MF (1998) Chondrogenic differentiation of cultured human mesenchymal stem cells from marrow. *Tissue Eng* **4**, 415–428.

Marcus AJ, Coyne TM, Rauch J, Woodbury D, Black IB (2008) Isolation, characterization, and differentiation of stem cells derived from the rat amniotic membrane. *Differentiation* **76**, 130–144.

McCarty RC, Gronthos S, Zannettino AC, Foster BK, Xian CJ (2009) Characterisation and developmental potential of ovine bone marrow derived mesenchymal stem cells. *J Cell Physiol* **219**, 324–333.

Meirelles LDA S, Nardi NB(2003)Murine marrow-derived mesenchymal stem cell: isolation, in vitro expansion, and characterization. *Br J Haematol*, **123**, 702–711.

Mori M, Sadahira Y, Awai M (1987) Characteristics of bone marrow fibroblastic colonies (CFU-F) formed in collagen gel. *Exp Hematol* **15**, 1115–1120.

Nadri S, Soleimani M, Hosseni RH, Massumi M, Atashi A, Izadpanah R (2007) An efficient method for isolation of murine bone marrow mesenchymal stem cells. *Int J Dev Biol* **51**, 723–729.

Neagu M, Suciu E, Ordodi V (2005) Human mesenchymal stem cells as basic tools for tissue engineering: isolation and culture. *Romanian J Biophys* **15**, 29–34.

Neuhuber B, Swanger SA, Howard L, Mackay A, Fischer I (2008) Effects of plating density and culture time on bone marrow stromal cell characteristics. *Exp Hematol* **36**, 1176–1185.

Neupane M, Chang CC, Kiupel M, Yuzbasiyan-Gurkan V (2008) Isolation and characterization of canine adipose-derived mesenchymal stem cells. *Tissue Eng Part A* **14**, 1007–1015.

Owen ME, Cave J, Joyner CJ (1987) Clonal analysis in vitro of osteogenic differentiation of marrow CFU-F. *J Cell Sci* **87**(Pt 5), 731–738.

Raimondo S, Penna C, Pagliaro P, Geuna S (2006) Morphological characterization of GFP stably transfected adult mesenchymal bone marrow stem cells. *J Anat* **208**, 3–12.

Rebelatto CK, Aguiar AM, Moretao MP, et al. (2008) Dissimilar differentiation of mesenchymal stem cells from bone marrow, umbilical cord blood, and adipose tissue. *Exp Biol Med (Maywood)* **233**, 901–913.

Sahoo S, Ang LT, Cho-Hong Goh J, Toh SL (2010)Bioactive nanofibers for fibroblastic differentiation of mesenchymal precursor cells for ligament/tendon tissue engineering applications. *Differentiation*, **79**, 102–110.

Schellenberg A, Lin Q, Schuler H, et al. (2011) Replicative senescence of mesenchymal stem cells causes DNA-methylation changes which correlate with repressive histone marks. *Aging (Albany NY)* **3**, 873–888.

Sekiya I, Larson BL, Smith JR, Pochampally R, Cui JG, Prockop DJ (2002) Expansion of human adult stem cells from bone marrow stroma: conditions that maximize the yields of early progenitors and evaluate their quality. *Stem Cells* **20**, 530–541.

Selvaratnam L, Abd Rahim S, Kamarul T, et al. (2005)Colonies in engineered articular cartilage express superior differentiation. *Med J Malaysia* **60**, Suppl C, 49–52.

Seo MS, Jeong YH, Park JR, et al. (2009) Isolation and characterization of canine umbilical cord blood-derived mesenchymal stem cells. *J Vet Sci* **10**, 181–187.

Smith JR, Pochampally R, Perry A, Hsu SC, Prockop DJ (2004) Isolation of a highly clonogenic and multipotential subfraction of adult stem cells from bone marrow stroma. *Stem Cells* **22**, 823–831.

Tan S. L., Ahmad R. E., Ahmad T. S., et al. (2012) Effect of growth differentiation factor 5 on the proliferation and tenogenic differentiation potential of human mesenchymal stem cells in vitro. *Cells Tissues Organs* **196**, 325–338.

Tan SL, Sulaiman S, Pingguan-Murphy B, Selvaratnam L, Tai CC, Kamarul T (2011) Human amnion as a novel cell delivery vehicle for chondrogenic mesenchymal stem cells. *Cell Tissue Bank* **12**, 59–70.

Tay LX, Ahmad RE, Dashtdar H, et al. (2011) Treatment outcomes of alginate-embedded allogenic mesenchymal stem cells vs. autologous chondrocytes for the repair of focal articular cartilage defects in a rabbit model. *Am J Sports Med* **40**, 83–90.

Taylor SE, Smith RK, Clegg PD (2007) Mesenchymal stem cell therapy in equine musculoskeletal disease: scientific fact or clinical fiction? *Equine Vet J* **39**, 172–180.

Tropel P, Noel D, Platet N, Legrand P, Benabid AL, Berger F (2004) Isolation and characterisation of mesenchymal stem cells from adult mouse bone marrow. *Exp Cell Res* **295**, 395–406.

Varma MJ, Breuls RG, Schouten TE, et al. (2007) Phenotypical and functional characterization of freshly isolated adipose tissue-derived stem cells. *Stem Cells Dev* **16**, 91–104.

Warden SJ (2007) Animal models for the study of tendinopathy. *Br J Sports Med* **41**, 232–240.

Zeng L, Rahrmann E, Hu Q, et al. (2006) Multipotent adult progenitor cells from swine bone marrow. *Stem Cells* **24**, 2355–2366.

Supporting Information

Additional Supporting Information may be found in the online version of this article:

Table S1 Basic demographics and the origin of tissue samples (both for hMSCs and the primary native hTeno cultures) from the donors.

Fig. S1. Comparison of rbMSCs and hMSCs phenotypic expression.

Fig. S2. Expression of CD105, CD166, CD14 and CD19 on hMSCs.